INFLUENCE OF CARBON NANOTUBES AND GRAPHENE ON THERMAL AND ELECTROMAGNETIC PROPERTIES OF PLA NANOCOMPOSITES

Assist. Prof. Angelova P.[1*], Prof. D.Sc. Dr. Kotsilkova R.[1], Prof. Dr. Kuzhir P.[2]

[1] Institute of Mechanics (OLEM), Bulgarian Academy of Sciences, Bulgaria
[2] Institute for Nuclear Problems, Belarusian State University, Belarus
polq_s_angelova90@abv.bg

Abstract: *This work investigate electromagnetic and thermal properties of poly(lactic) acid-based composites with graphene nanoplates (GNP) and multiwalled carbon nanotubes (MWCNTs), produced by solution blending method. It was found that the MWCNT carbon nanotubes are an effective filler for both absorption and reflection of electromagnetic waves in the GHz and THz frequency domains. The higher aspect ratio of carbon nanotubes, compared to industrial MWCNT, is the cause of better electromagnetic characteristics of nanocomposites prepared by solution blending method (SB). The DSC analysis of the samples shows that the glass transition is around 60^{o}C, followed by cold crystallization with enthalpy and melting temperature around 150^{o}C. The TGA analysis show, that the thermal stability of PLA polymer is improved by addition of 6% MWCNTs and GNP.*

KEYWORDS*: BIODEGRADABLE POLY(LACTIC ACID) NANOCOMPOSITES, GRAPHENE, CARBON NANOTUBES, ELECTROMAGNETIC PROPERTIES, THERMAL STABILITY*

1. Introduction

Poly (lactic acid) (PLA) is a plant-derived biodegradable polymer, which can be obtained from natural source such as corn starch and may be a sustainable alternative to petrochemical-derived polymers [1]. As a thermoplastic and aliphatic polyester, PLA has been used to produce beverage packages, biomedical supplies, food wares, vehicle interiors, films, and fibers [2,3]. Unfortunately, some significant disadvantages of PLA such as relatively poor mechanical properties, slow crystallization rate, and low thermal stability hinder its applications for more demanding requirements [4,5].

Carbon-based fillers such as carbon nanotubes (CNTs), nanofibers (CNFs) and graphene possess excellent electrical conductivity together notable mechanical and thermal properties [6,7,8]. When such nanoparticles are introduced in host polymeric matrices, the interesting properties of these latter (like easy processability and shaping possibilities, resistance to corrosion, flame, moisture, etc.), are enhanced giving rise to nanocomposites that recently have gained great attention from both academicians and industries. In fact, these innovative composites can leverage many of combined properties leading to develop new materials for several applications ranging from aeronautic, automotive, plastics, semiconductor and electronic industrial sectors [9,10].

In the present work we investigate binary and ternary composites based on PLA with graphene nanoplatelets and multiwall carbon nanotubes, produced by solution blending techniques. The electromagnetic interference (EMI) shielding effectiveness are determined by material absorptivity, surface reflectivity, and multiple internal reflections. Polymer films incorporating graphene and other nanocarbon fillers were recently studied as a light coating material to protect micro- and nano-devices in a harsh electromagnetic environment, due to the promising electromagnetic shielding efficiency of the carbon nanostructures [11,12]. The electromagnetic shielding of a composite material with carbon nanofillers, such as graphene nanoplatelets and carbon nanotubes, are studied mainly depend on the filler's intrinsic conductivity, dielectric constant and aspect ratio [13]. Thermal analysis are used to determinate thermal stability and degradation of the polymer and nanocomposites.

2. Materials and methods:

The poly(lactic) acid polymer (PLA) Ingeo 700 1D was used for the solution blending samples. Graphene nanoplates (GNP) and multiwall carbon nanotubes (MWCNT) produced by Times Nano, China were used for preparation of nanocomposites. The PLA types and different grades of GNP and MWCNTs are shown in Table 1.

Table 1. Typical properties of row materials used in this study

CNTs	GNPs
OD: >50nm	Layers <20
Length 1-5μm	Size D(0.5)=5-10μm
Purity: >95%	Purity > 99.5wt%

2.2. Methods of preparation of solution blending:

The TNGNP and MWCNTs were supplied from Times Nano, China. Ten types of compositions, combining different proportions of TNGNPs and MWCNTs were produced at maximum 6 wt% filler contents. The compositions were produced in laboratory OLEM, Bulgaria, Sofia.

Procedure for nanocomposite preparation: The PLA700 1D was dissolved in chloroform in ratio 1:3. Suspensions of graphene (TNGNP) and MWCNTs were prepared in 200 ml. chloroform by ultrasonic mixing and added to the dissolved PLA. The final mixture was mechanically stirred for 60 minutes and dried in a vacuum oven for 24 hours at 70 ^{o}C. Compositions with 1.5%, 3% and 6 wt% of TNGNP, and MWCNT and their combinations, in PLA were prepared by this solution blending technique.

2.3 Methods for characterization:

2.3.1 THz frequency range:

THz measurements were carried out using a commercial THz time-domain spectrometer shown on Fig. 1 [1]. A 1050±40 nm wavelength pumping laser having 50–150 fs pulse duration and more than 40 mW output power at approximately 80 MHz pulse repetition rate was used to excite a photoconductor antenna and produced THz radiation up to 2 THz. The layout of the system is shown on Fig. 1(b). The spectrometer, THz emitter and detector consists of a micro strip antenna integrated with a photoconductor (low temperature grown GaBiAs) and silicon lens. The THz detector output is proportional to the instant electrical field strength of the THz pulse during the ultrashort pumping pulse. The Fourier transformation of waveform of electrical field of THz radiation gives the spectral content (E(x)) of THz radiation.

2.3.2 GHz frequency range:

The microwave measurements were provided by a scalar network analyzer R2-408R [fig.2] at room temperature and normal pressure. The scalar network analyzer is designed for measurement of the transmission factor and reflection factor module Voltage Standing Wave Ratio (VSWR) of waveguide devices and components in frequency range from 25.96 GHz to 37.5 GHz.

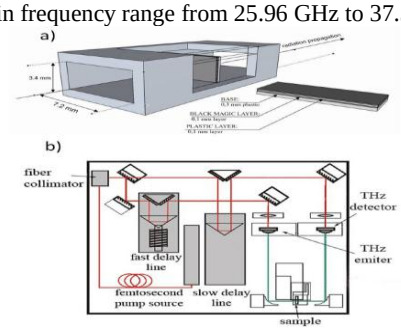

Fig. 1 The equipment for THz frequency range measurement

The frequency sweep bandwidth range can vary from the full frequency range of the instrument to 1500 MHz. Basic error limit of the frequency setting does not exceed ±0.2% in normal conditions. The frequency stability of the oscillator was controlled by a frequency meter and was as high as 10^{-6}. The power stabilization was maintained in the level of 7.0 mW ± 10 μW. EM attenuation was measured in the 0 db to -40 db.

The scalar network analyzer ELMIKA R2-408R

Fig.2 *The equipment for GHz frequency range measurement*

2.3.3 Differential scanning calorimetry (DSC Q20):

For the thermal properties measurements, a differential scanning calorimeter, DSC Q20, bought from the American company TA Instruments, shown in Figure 3, was used.

Technical characteristics of DSC Q20 (TA Instruments)
Temperature range - from room temperature to 725 ° C
Temperature Accuracy +/- 0.1°C
Temperature precision +/- 0.05°C
The experiments are carried out in an air atmosphere or in nitrogen.

The conditions under which the current DSC test was carried out were: a temperature range of 20 to 200 °C in a nitrogen atmosphere with a heating step of 20 ° C / min.

(a) (b)

Figure 3 a) DSC Q20 (TA Instruments), b) pan

2.3.4 Thermogravimetric analysis (TGA 50):

For the thermal properties measurements, a differential scanning calorimeter, TGA Q50, bought from the American company TA Instruments, shown in Figure 4, was used.

Technical characteristics of the TGA Q50 (TA Instruments):
Temperature range - from room temperature to 1000°C
Maximum sample weight - 1g
Weight precision - +/- 0.01%
Experiments are conducted in an air or nitrogen atmosphere.

The conditions under which the current TGA test was carried out are: heating the sample from 20 to 500 °C under nitrogen, with a heating step of 20 ° C / min.

3. Results and Discussion:

3.1 Electromagnetic properies in THz frequency range:

Table 2 show that for ternary nanocomposites containing MWCNT and GNP show the highest electromagnetic shielding efficiency (EMI) of 97-100%. Due to high reflection of 53% and a very high absorption value of 47% the trinary composite 4.5%GNP/1.5%MWCNT achieves the highest EMI of 100%. The pure PLA matrix has the smallest value of EMI shielding due to a high transmission. It is obvious that in ternary composites, the reflection and absorption decrease with decreasing of amount of MWCNT (Fig.4). For the binary composites, the graphene composite (6wt% GNP/PLA) achieve the highest 96% EMI shielding, due to high reflection (52%) and high absorption (44%) and transmission only 4%. The 6% MWCNT/GNP has the lowest value EMI of 62% in THz range.

Table 2: *The results for THz frequency, solution blending for reflection-transmission-absorption (R-T-A) in range 0.2 – 0.6 THz*

No.	Content of filler [wt%]	Thickness [mm]	R-mid	T-mid	A-mid 1-R-T	EMI [%]
1	PLA	1.07	0.30	0.79	0	30
2	6% GNP/PLA	0.84	0.52	0.04	0.44	96
3	6%MWCNT/PLA	0.89	0.32	0.38	0.30	62
4	1.5%GNP/4.5% WCNT/PLA	0.97	0.48	0.03	0.49	97
5	3%GNP/3% MWCNT/PLA	0.76	0.55	0.02	0.43	98
6	4.5%GNP/1.5% MWCNT/PLA	0.97	0.53	0	0.47	100

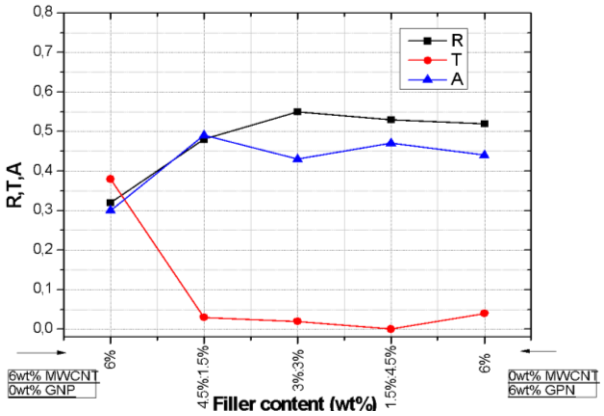

Fig. 4 *The comparison of electromagnetic response (reflection/transmission/absorption coefficients) at 0.3 THz of 1-mm thick samples with different MWCNT- and GNP-content*

3.2. Electromagnetic properies in GHz frequency range:

Table 3 and Figure 5 present the electromagnetic properties of the 6wt% binary and ternary nanocomposites in the GHz wave range.

Table 3: The results for 32.5 GHz frequency, solution blending for reflection-transmission-absorption (R-T-A)

No	Content of filler, [wt%]	Thickness [mm]	R	T	A-mid	EMI [%]
1	PLA	1	0.25	0.75	0.003	25
2	6% GNP/PLA	1	0.47	0.15	0.38	85
3	6% MWCNT/PLA	0.93	0.44	0.40	0.16	60
4	1.5%GNP/4.5%MWCNT/ PLA	0.96	0.67	0.19	0.14	81
5	3%GNP/3% MWCNT/ PLA	0.99	0.41	0.28	0.31	72
6	4.5%GNP/1.5%MWCNT/ PLA	0.94	0.50	0.09	0.41	91

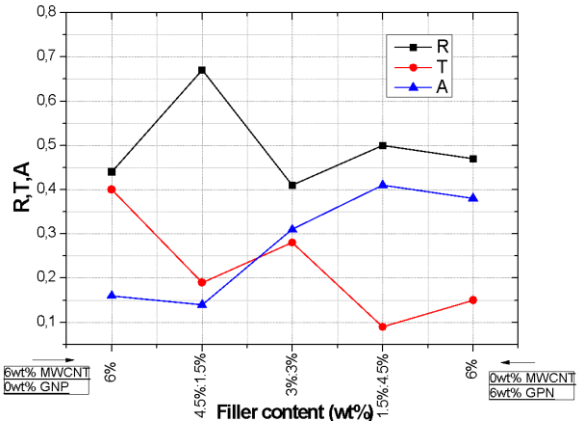

Figure 5 *Comparison of reflection/transmission/absorption coefficients of 1-mm thick composite at 32.5 GHz with different mixtures of MWCNT and GNP.*

In the GHz frequency range, the graphene composites (6wt% GNP/PLA) achieve higher EMI shielding (85%), compared to that of the binary composite 6wt% MWCNT/PLA (60%). In the ternary nanocomposites, both absorption and reflection are higher than those of binary composites, which speaks for synergy in the properties generated by the combination of the two carbon nanoparticles. The highest EMI shielding (91%) in the GHz zone is observed for bi-filler composites with a combined content of filler of 4.5wt% GNP / 1.5wt% MWCNT / PLA, where high absorption (41%) and high reflection (50%) are achieved (Table 3).

3.3. DSC Analysis:

This study was helpful to understand a shelf-life of the samples during storage in room conditions, related with the PLA degradation due to the exposure to humidity and UV light. First step was to measure fresh samples and after that we measured the same samples after 18 months storage in room conditions. The Table 4 summarize the DSC determined specific temperatures for glass transition (Tg), cold crystallization (Tcc) and melting (Tm), as well as the enthalpies of crystallization and melting (ΔHcc and ΔHm). Figure 6 compares the DSC thermodiagrames from the first run of fresh samples and samples after 18 months storage in room conditions.

Table 4 *Results from DSC analysis for two type samples – fresh samples and after 18 months storage samples.*

Name of the fresh samples	**DSC result of the fresh samples**					
	Tg, °C	**Tcc, °C**	**Tm, °C**	**ΔHcc, J/g**	**ΔHm, J/g**	**χc, %**
PLA	50.0	104.3	144.4	13.5	17.3	4.1
6% GNP/PLA	54.1	119.3	147.0	12.6	13.2	0.7
6% MWCNT/PLA	49.8	105.3	144.8	10.2	15.3	5.8
3%GNP/3% MWCNT/PLA	52.4	117.3	145.8	6.2	12.1	6.7
1.5%GNP/4.5% MWCNT/PLA	53.1	110.2	146.2	7.6	14.0	7.3
4.5%GNP/1.5% MWCNT/PLA	52.0	113.2	145.7	8.6	13.5	5.6
Name of the storage samples	**DSC results of the 18m storage**					
	Tg, °C	**Tcc, °C**	**Tm, °C**	**ΔHcc, J/g**	**ΔHm, J/g**	**χc, %**
PLA	62.6	119.4	148.5	5.8	9.1	3.5
6% GNP/PLA	62.3	-	148.1	-	2.8	3.3
6% MWCNT/PLA	61.3	127.3	146.5	0.6	2.6	2.4
3%GNP/3% MWCNT/PLA	63.7	123.5	148.7	1.8	5.0	3.7
1.5%GNP/4.5% MWCNT/PLA	61.7	125.3	146.8	0.8	3.5	3.1
4.5%GNP/1.5% MWCNT/PLA	63.9	119.8	150.2	4.5	11.0	7.4

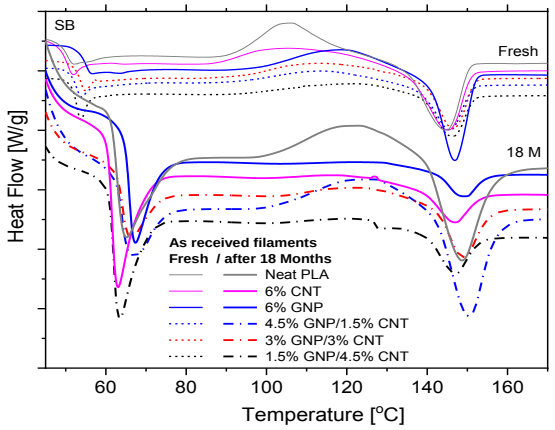

Fig. 6 *Comparison of DSC curves between binary (GNP/PLA, MWCNT/PLA) and ternary (GNP/MWCNT/PLA) composites investigated as fresh samples and after 18 months storage*

From DSC analysis (Table 4) for the both type of samples (fresh and after 18 months) the binary composites of 6% GNP show higher temperatures of crystallization and melting compared with the same amount of MWCNT. Cold crystallization peak increase with (15°C) for fresh samples and (8°C) for samples after 18 months, if compare with pure PLA (104°C) and (119.4), respectively. For ternary composites 1.5% GNP/4.5% MWCNT from fresh samples has the biggest % of crystallinity which is comparable with 4.5%GNP/1.5%MWCNT from samples after 18 months storage. The peaks of cold crystallization and melting are shifted on the right side due to the higher temperature for samples after 18 months storage. Generally, glass transition temperature has increased with ~ 9 °C for samples after 18 months storage. The binary composite with 6wt% GNP has the higher temperature of glass transition for both type of samples (fresh and after 18 months storage) which is indicated that this temperature doesn't change with the time and storage of the samples. For ternary composites it is obvious that with decreasing filler content of MWCNT Tg is increased (for fresh samples) and decreased for samples investigate after 18 months (table 4). The crystallinity also decreases – for fresh samples it is around 4% for near PLA matrix and 6-7% for the nanocomposites after 18 months storage due to some nucleation effect of nanofillers on PLA, resulting in α′–α phase transition. Almost twice decrease of the % crystallinity (to 2-3%) is observed in the aged filaments if compared with the fresh prepared one.

From those result it can be concluded that thermal characteristics, like of glass transition, crystallization and melting were enhanced for these samples after 18 months storage (Fig. 6). The % crystallinity is slightly decreased for some compositions confirming very slight effect of PLA degradation at room storage conditions.

3.4 TGA Analysis:

The TGA analysis was used to determine the thermal stability and degradation of the PLA-based binary and ternary composites with GNP and MWCNTs. Results are presented in Fig. 7 and Table 5.

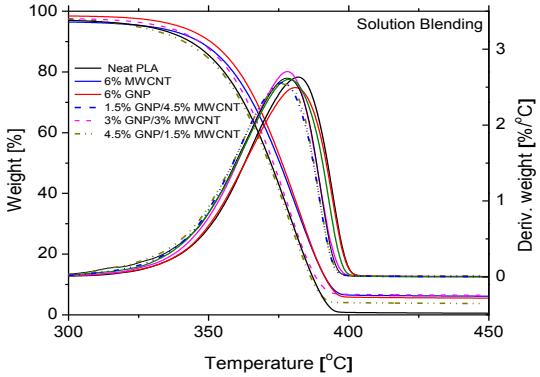

Fig.7 *TGA curve weight vs temperature for nanocomposites with maximum of 6wt% nanofiller (GNP, MWCNT and mixed)*

Table 5 *The values of T_{onset} , $T_{10\%}$, peak of degradation, mass loss at 105°C, and residue ash at 490°C for binary (GNP/PLA, MWCNT/PLA) and ternary (GNP/MWCNT/PLA) composite prepared by solution blending method.*

Name	T_{onset} [°C]	$T_{10\%}$ [°C]	Peak of degr. T_p °C]	Mass of loss at 105°C [%]	Residue ash at 490 °C, [%]
PLA	304.5	343.0	378.6	0.3	0.5
6%GNP/ PLA	314.3	350.3	382.3	0.2	5.4
6%MWCNT/ PLA	311.4	346.5	380.6	0.3	6.0
1.5 %GNP/ 4.5%MWCNT	313.0	344.3	378.9	0.4	4.7
1.5%GNP/ 4.5% MWCNT/ PLA dried	310.5	342.4	376.2	0.3	6.1
3%GNP/ 3%MWCNT/PLA	308.3	346.5	378.3	0.3	6.3
4.5%GNP/ 1.5%MWCNT/PLA	289.5	340.8	361.1	0.3	2.6
4.5%GNP/ 1.5%MWCNT/ PLA dried	289.5	340.2	376.9	0.3	3.0

TGA analysis (fig. 2b) show that the binary nanocomposite with graphene, 6% GNP/PLA has the highest values for the three measured temperatures: Tonset (314°C), T10% (350° C) and Tp (382°C). Mass loss at 105°C is lowest for this composite (0.2wt%), which indicates that graphene nanoplates are as barriers for heating. Binary composite with 6% MWCNT/PLA has only 3-4°C lower thermal stability than the composite with 6% GNP. The thermal stability of ternary nanocomposites is slightly lower than that of binary systems. The T_{onset} (initial degradation) also increases with 4°C from pure PLA to 4.5%GNP/1.5wt%MWCNT. Residue ash increases with 7% from pure PLA to 3wt%GNP/3wt%MWCNT. Two nanocomposites were additional dried. For ternary nanocomposites with 4.5% GNP/1.5% MWCNT shows that thermal stability is improved with 16°C and shifted on the right side due to higher temperature compared to the same sample that is not dried (table 5). The other nanocomposite 1.5% GNP/4.5% MWCNT shows that the additional dried sample has lower values (2-3°C) for all characteristics compared with not dried sample.

4. Conclusion:

The binary and ternary composites based on PLA filled with 6 wt% GNP and MWCNTs prepared by solution blending are studied here with. Good electromagnetic and thermal properties are obtained as varying the filler ratios.

The graphene nanoplatelets (GNP) in PLA composites are a more efficient EMI absorbing filler than MWCNT in both GHz and THz frequency ranges for the 6wt% filled binary nanocomposites produced by solution blending technique.

For binary composites with 6 wt.% GNP, about 85% EMI shielding is achieved due to a high reflection of 47% but also a relatively high absorption of 38%. These composites show different behavior at reflection / transmission/ absorption rates compared to carbon nanotubes. As the content of the filler increases, the transmission gradually decreases, reaching the lowest value of 15% at 6%GNP when filling the system up to the maximum.

In ternary nanocomposites - absorption and reflection are higher than those of binary, which speaks for synergy in the properties produced by the combination of the two carbon nanoparticles. The highest level of EMI shielding (91%) in GHz is observed in combined ternary compositions with 4.5%GNP/1.5% MWCNT, where high absorption (41%) and high reflection (50%) are achieved.

The fresh produced filaments were compared with the aged filaments after 18 months storage in room conditions. A nucleation effect of graphene and carbon nanotubes on the crystal structure of PLA was observed. Our findings confirm that the % crystallinity of the fresh extruded filaments is about 4% for the neat PLA and 6-7% for the nanocomposites due to some nucleation effect of nanofillers on PLA, resulting in recrystallization, producing α′–α phase transition. Almost twice decrease of the % crystallinity (to 2-3%) is observed in the aged filaments if compared with the fresh prepared one. The effects was associated with structural changes in the PLA biopolymer due to the long-term exposure to humidity, UV light and temperature, typical for room storage environment. Different nucleation effects are observed for both GNP and MWCNT fillers.

The nanocomposite content 6% GNP has the lowest (0.2%) mass of loss at 105°C. This show that graphene nanoplatelets are well dispersed and they are a barrier for heat distribution and exposure to humidity into the nanocomposite. The binary nanocomposite with 6% MWCNT has a lower thermal stability (3-4°C) compare with 6% GNP. The lowest thermal stability has a ternary nanocomposite 4.5% GNP/1.5% MWCNT (17°C compare with pure PLA). In general thermal stability decreases with the decreasing the MWCNT content for the ternary nanocomposites, possibly as a results of a bad dispersion of the fillers.

Acknowledgments: This work was supported by the European projects H2020-MSCA-RISE-2016-734164 Graphene 3D and H2020-SGA-FET-GRAPHENE-2017-785219 Graphene Core2.

5. References

[1] Saeidlou S., Huneault M.A, Li H., Park C.B., "Poly (lactic acid) crystallization" Prog. Polym. Sci. 37 (2012) 1657e1677.
[2] Savaris M., Santos V.D., Brandalise R.N., "Influence of different sterilization processes on the properties of commercial poly(lactic acid)", Mater. Sci. Eng. C 69 (2016) 661e667.
[3] Yang F., Murugan R., Ramakrishna S., Wang X., Ma Y.X., Wang S., "Fabrication of nano-structured porous PLLA scaffold intended for nerve tissue engineering", Biomaterials 25 (2004) 1891e1900.
[4] Aou K., Hsu S.L., Kleiner L.W., Tang F.-W., "Roles of conformational and configurational defects on the physical aging of amorphous poly(lactic acid)", J. Phys. Chem. B 111 (2007) 12322e12327.
[5] Tsuji H., Fukui I. " Enhanced thermal stability of poly (lactide) s in the melt by enantiomeric polymer blending", Polymer 44 (2003) 2891e2896.
[6] Spinelli G, Lamberti P, Tucci V, Ivanova R, Tabakova S, Ivanov E, Kotsilkova K, Cimmino S, Maio R, Silvestre C, "Rheological and electrical behaviour of nanocarbon/poly(lactic) acid for 3d printing applications" , addma_2018_122.
[7] Zhang W., Dehghani-Sanij A.A, and Blackburn R. S. "Carbon based conductive polymer composites", J. Mater. Sci. 42 (2007) 3408-3418.
[8] Cha J., Jun G. H., Park J. K, Kim J. C., Ryu H. J., Hong S. H., "Improvement of modulus, strength and fracture toughness of CNT/Epoxy nanocomposites through the functionalization of carbon nanotubes", Compos. Part B 129 (2017) 169-179.
[9] Vertuccio L., Guadagno L., Spinelli G., Russo S., Iannuzzo G., "Effect of carbon nanotube and functionalized liquid rubber on mechanical and electrical properties of epoxy adhesives for aircraft structures", Compos. Part B 129 (2017) 1-10.
[10] Guadagno L., Raimondo M., Vittoria V., Vertuccio L., Naddeo C., Russo S., De Vivo B., Lamberti P., Spinelli G. and Tucci V., "Development of epoxy mixtures for application in aeronautics and aerospace" RSC Adv. 4 (2014) 15474-15488.
[11] Qin F. and Brosseau C., " A review and analysis of microwave absorption in polymer composites filled with carbonaceous particles" ,J. Appl. Phys. 111, 061301 (2012).
[12] Kuzhir P., Paddubskaya A., "Epoxy composites filled with high surface area-carbon fillers: Optimization of electromagnetic shielding, electrical, mechanical, and thermal properties", Plyushch A. et al., J. Appl. Phys. 114, 164304 (2013).
[13] Bryning M.B, Islam M.F, Kikkawa J.M, Yod A.G, "Preparation and Microwave Absorbing Characteristics of Multi-Walled Carbon Nanotube/Chiral-Polyaniline Composites", Adv Mater, 17, 9 (2005). http://dx.doi.org/10.1002/adma.200401649.